Proteomic Analysis of the Bovine and Human Ciliary Zonule

Alicia De Maria,[1] Phillip A. Wilmarth,[2] Larry L. David,[2] and Steven Bassnett[1]

[1]Ophthalmology and Visual Sciences, Washington University School of Medicine, St. Louis, Missouri, United States
[2]Biochemistry and Molecular Biology, Oregon Health and Science University, Portland, Oregon, United States

Correspondence: Steven Bassnett, Department of Ophthalmology and Visual Sciences, Washington University School of Medicine, 660 S. Euclid Avenue, Box 8096, St. Louis, MO 63110 USA;
bassnett@vision.wustl.edu.

Submitted: October 4, 2016
Accepted: November 29, 2016

Citation: De Maria A, Wilmarth PA, David LL, Bassnett S. Proteomic analysis of the bovine and human ciliary zonule. *Invest Ophthalmol Vis Sci*. 2017;58:573–585. DOI:10.1167/iovs.16-20866

Purpose. The zonule of Zinn (ciliary zonule) is a system of fibers that centers the crystalline lens on the optical axis of the eye. Mutations in zonule components underlie syndromic conditions associated with a broad range of ocular pathologies, including microspherophakia and ectopia lentis. Here, we used HPLC–mass spectrometry to determine the molecular composition of the zonule.

Methods. Tryptic digests of human and bovine zonular samples were analyzed by HPLC–mass spectrometry. The distribution of selected components was confirmed by immunofluorescence confocal microscopy. In bovine samples, the composition of the equatorial zonule was compared to that of the hyaloid zonule and vitreous humor.

Results. The 52 proteins common to the zonules of both species accounted for >95% of the zonular protein. Glycoproteins constituted the main structural components, with two proteins, FBN1 and LTBP2, constituting 70%–80% of the protein. Other abundant components were MFAP2, EMILIN-1, and ADAMTSL-6. Lysyl oxidase-like 1, a crosslinking enzyme implicated in collagen and elastin biogenesis, was detected at significant levels. The equatorial and hyaloid zonular samples were compositionally similar to each other, although the hyaloid sample was relatively enriched in the proteoglycan opticin and the fibrillar collagens COL2A1, COL11A1, COL5A2, and COL5A3.

Conclusions. The zonular proteome was surprisingly complex. In addition to structural components, it contained signaling proteins, protease inhibitors, and crosslinking enzymes. The equatorial and hyaloid zonules were similar in composition, but the latter may form part of a composite structure, the hyaloid membrane, that stabilizes the vitreous face.

Keywords: lens, zonule, zonulome, LTBP2, FBN1, hyaloid, vitreous, matrisome

The zonule of Zinn, named for the German anatomist who first described it,[1] is a system of radial extracellular fibers that interconnects the ciliary body and the crystalline lens (Fig. 1). The fibers, which in humans are several millimeters in length and approximately 50 μm in diameter,[2] transmit the forces that flatten the lens during disaccommodation, the process by which distant objects are brought into focus. In nonaccommodating species, the zonule ensures proper centration of the lens on the optical axis.[3] Zonular fibers emerge from the surface of the pars plana region of the nonpigmented ciliary epithelium and project forward toward the lens, passing through the folds of the ciliary processes in the pars plicata. As they near the lens, the fibers splay. Most attach directly to the equatorial lens surface, but a subset of fibers, the hyaloid zonule, runs for some distance across the vitreous face (Fig. 2) before terminating on the posterior lens capsule at or near Egger's line.[4]

The primary function of zonular fibers is mechanical, and a number of studies have analyzed their material properties. The fibers are relatively elastic, able to stretch up to four times their original length before breaking, although elasticity declines markedly with age.[5] The elastic modulus of the zonule has been variously reported as 0.35,[6] 0.27–0.34,[7] and 1.5 MPa.[8] Electron microscopy indicates that zonular fibers are composed exclusively of bundles of microfibrils.[9] Atomic force measurements on individual microfibrils suggest that they are relatively stiff structures, with a modulus of 80–100 MPa.[10] Thus, the elasticity of the intact zonule (two orders of magnitude greater than that of the component microfibrils) is presumably attributable to reversible changes in the supramolecular organization of the bundles. In other model systems, notably the sea cucumber dermis, the strength of microfibrillar networks has been attributed to the presence of nonreducible crosslinks, whereas their elasticity appears to depend on disulfide bonds.[11]

Elsewhere in the body, microfibrils are common constituents of the extracellular matrix (ECM). They occur as individual fibrils 10–12 nm in diameter or as part of collective structures, such as the mantle covering the surface of elastin-rich elastic fibers. The microfibril bundles in the ciliary zonule are somewhat unusual in that they are not associated with elastin. The main constituent of microfibrils is fibrillin-1 (FBN1), a 350-kDa glycoprotein.[12] Microfibrillar-associated protein 2 (MFAP-2, aka MAGP1) is another ubiquitous microfibril component.[13] Both FBN1 and MFAP2 were detected in an early mass spectrometry study of the human zonular proteome.[14]

Because the zonule constitutes a relative pure population of elastin-free microfibrils and can be isolated without resorting to lengthy purification protocols, it offers an opportunity to identify other, perhaps less abundant, microfibril components.

Investigative Ophthalmology & Visual Science

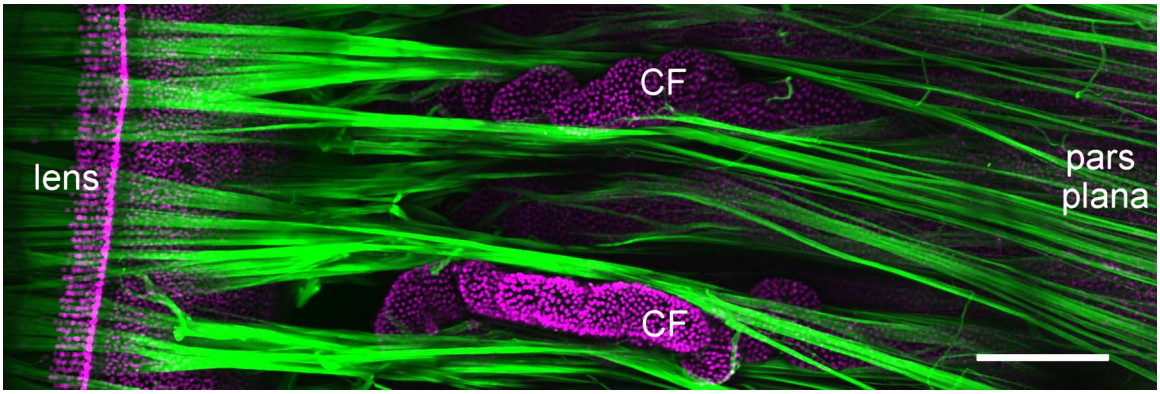

Figure 1. Zonule structure in a primate (baboon) eye viewed from the posterior aspect. The zonule (*green*) was visualized by confocal microscopy after incubation with anti-MFAP2 (see Ref. 3 for methodology). Zonular fibers project from the pars plana region of the nonpigmented ciliary epithelium, pass between the ciliary folds (CF) of the pars plicata, and terminate on the lens surface near the equator. *Scale bar* denotes 250 μm.

Work from several laboratories suggests that the composition of the zonule may be quite complex. For example, immunofluorescence analysis of the zonule detected two other members of the fibrillin family, FBN2 and FBN3,[15] as well as a structurally related protein, latent TGFβ-binding protein 2 (LTBP2).[16] Furthermore, it is possible, perhaps even likely, that zonule fibers are not uniform in composition. The hyaloid zonule, for example, may differ from the equatorial zonule. We can also anticipate that specific protein interactions are required to anchor the ends of the zonular fibers to the lens or the ciliary epithelium and that these may be reflected in uneven protein distributions along the length of fibers. An example may be ADAMTSL-4, a putative zonule component, which has been proposed to anchor zonular fibers to the lens capsule and may therefore be enriched in the proximal portion of the fibers.[17]

As well as serving as a useful model system for studying microfibril organization, the composition of the zonule is of interest in its own right. Increased zonular fragility is a feature of aging[18] and a hallmark of several systemic or ophthalmic diseases. In exfoliation syndrome, for example, the zonular fibers are weakened, resulting in phacodonesis and subluxation of the lens, or even frank zonulysis.[19,20] Systemic metabolic disorders, such as homocystinuria, commonly result in lens dislocation (ectopia lentis) secondary to disintegration of zonular fibers. In isolation, ectopia lentis is associated with mutations in *ADAMTSL-4,*[21,22] but is also observed in syndromes resulting from mutations in genes such as *FBN1* (Marfan syndrome; MIM:154700) and *LTBP2* (Weill-Marchesani syndrome type 3; MIM:614819). Elucidating the zonule proteome ("zonulome") will help us better understand the contribution that individual components make to the overall mechanical properties of the fibers and their long-term stability.

In the current study, we analyzed the zonulome in humans and cows, verifying the location of several newly identified components by immunofluorescence. We also performed a comparative analysis of the anterior zonule, hyaloid zonule, and vitreous humor from the bovine eye.

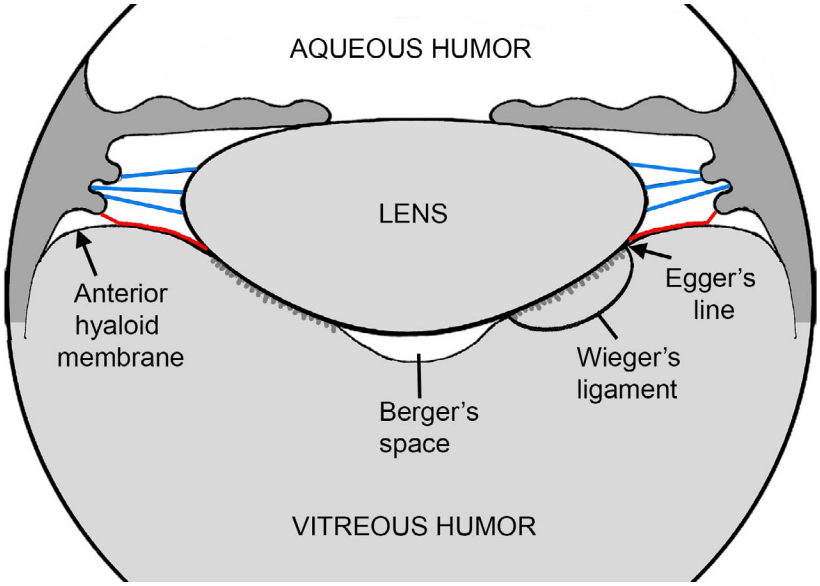

Figure 2. Schematic representation of the spatial relationship between the lens, ciliary zonule, anterior hyaloid membrane, and the vitreous humor. Equatorial zonular fibers (*blue*) project from the ciliary body to the lens. Fibers from the hyaloid zonule (*red*) are closely associated with the anterior face of the vitreous (the anterior hyaloid membrane) and make contact with the lens at Egger's line. Wieger's ligament is a region of tight adhesion between the posterior lens capsule and the vitreous humor. In humans, this attachment sometimes weakens with age, leading to the formation of a virtual space (Berger's space) between the back surface of the lens and the vitreous humor.

Investigative Ophthalmology & Visual Science

Table. Description of Human Zonular Samples

Sample No.	Sex	Age, y	Number of Eyes
1	Male	46	2
2	Male	54	2
3	Female	49	2
4	Female	55	2
5	Male	23	1
6	Male	54	2
7	Male	64	1
8	Female	48	1
9	Male	66	1
10	Female	23	2

Materials and Methods

Zonule Dissection

Bovine eyes (from 3-year-old animals) were obtained from a local slaughterhouse within 3 hours of death. The eye globe was dissected from its anterior aspect, the cornea and iris were removed, and the front face of the ciliary processes was exposed. The lens, zonule, and ciliary body were released from the eye and transferred to a Petri dish filled with Ringer's solution. We divided the zonular fibers into two groups: the "equatorial zonule" (blue fibers in Fig. 2) and the "hyaloid zonule" (red fibers in Fig. 2). The equatorial zonule was composed of fibers that projected directly to the lens surface. Other investigators[4] have subdivided these fibers into anterior, equatorial, and posterior groupings, but here they were all included in a single sample, the equatorial zonule. Using iridectomy scissors, fibers from the equatorial zonule were first transected near the ciliary body and then grasped with fine forceps and cut close to the lens. Because the equatorial fibers are anatomically isolated within the eye, it was possible to remove them precisely, with little or no contamination from other tissues. Once the equatorial fibers had been removed, the "hyaloid zonule" was exposed. The hyaloid zonule was defined as the set of fibers that were closely associated with the anterior face of the vitreous. They were also significantly longer than the equatorial fibers. Because they were intimately connected to the vitreous face, it was not possible to dissect the hyaloid fibers as precisely as the equatorial fibers, and the hyaloid sample inevitably contained some elements of the anterior vitreous humor. The equatorial and hyaloid zonular fibers were collected separately into 1.5-mL microfuge tubes. Samples were centrifuged for 10 minutes at maximum speed, supernatants were removed, and the zonular pellet was frozen immediately. A third sample, taken from the center of the vitreous humor, was collected for comparative analysis. A single bovine eye yielded sufficient tissue for a proteomic analysis of the equatorial zonule, hyaloid zonule, and vitreous humor. We performed three such analyses using eyes from three different animals.

Human eyes (from 10 donors 23–66 years of age; Table) were obtained from a local eye bank and dissected using a similar approach to that described for the bovine eye. Because the vitreous of the aged human eye was often partially liquefied, it was not possible to collect a human hyaloid zonule sample. Thus, the human zonular sample was equivalent to the bovine equatorial zonule sample.

To have sufficient material for analysis, human zonular samples were pooled (Table). Pool A consisted of samples 1, 5, and 8. Pool B was samples 3 and 6. Pool C was samples 4, 7, and 9. Pool D was samples 2 and 10. Thus, each pool contained combined material from four eyes of both sexes, with mean ages ranging from 38.5 (pool D) to 60 years (pool C).

Histology and Immunofluorescence

Human eyes were fixed for 1 week in 4% paraformaldehyde/PBS, dehydrated through graded ethanols and xylene, and embedded in paraffin wax. Sections (4 μm thick) were cut in the midsagittal plane and processed for immunofluorescence. Deparaffinized sections were antigen retrieved using a 60°C overnight incubation in sodium citrate buffer (10 mM sodium citrate, 0.05% Tween-20; pH 6.0). Sections were blocked with 3% BSA for 2 hours and incubated overnight at 4°C in a 1:50–1:100 dilution of primary antibody. The following antibodies were used: ADAMTSL-6/THSD4 (Atlas Antibodies, Stockholm, Sweden), EMILIN-1 (Santa Cruz Biotechnology, Santa Cruz, CA, USA), FBN1 (Millipore, Temecula, CA, USA), fibulin-6/hemicentin-1 (Millipore), LTBP2 (gift of Tomoyuki Nakamura, Kansai Medical University, Osaka, Japan), and MFAP2 (Santa Cruz Biotechnology). After washing in PBS (3 × 10 minutes), sections were incubated for 2 hours in 1:300 dilution of appropriate secondary antibody (Alexa 488–conjugated goat anti-mouse or anti-rabbit; Invitrogen, Carlsbad, CA, USA) containing methyl green (a nuclear counterstain). Sections were then washed, coverslipped (Prolong Gold; Invitrogen), and viewed using an Olympus FV1000 confocal microscope (Center Valley, PA, USA).

Zonule Digestion

Bovine and human zonules were suspended in 50 μL buffer containing 4% SDS, 0.2% deoxycholic acid (DCA), and 100 mM ammonium bicarbonate (pH 8) and sonicated using a Fisher Scientific Model 60 Sonic Dismembranator (Thermo Fischer Scientific, Waltham, MA, USA), using three treatments of 10 seconds each. Samples were then shaken for 10 minutes at 600 RPM in a thermo-mixer at 90°C. Five microliters was removed for a Pierce bicinchoninic acid (BCA) assay (Thermo Fisher Scientific) using BSA as a standard. Five microliters of 0.5 M Tris (2-carboxyethyl)phosphine (TCEP) was then added, and the samples were heated at 90°C for an additional 10 minutes and centrifuged at 14,000*g* for 10 minutes, the supernatant was mixed with 200 μL exchange buffer containing 8 M urea, 0.2% DCA, and 100 mM ammonium bicarbonate, and the mixture was transferred to Tween-20 passivated Ultra-0.5 Centrifuge Filter Units (Amicon UFC503008; EMD Millipore, Billerica, MA, USA). The remaining sample preparation and digestion used the enhanced filter-aided sample preparation (eFASP) method of Erde et al.[23] Briefly, the SDS containing lysis buffer was replaced with exchange buffer, proteins were alkylated with iodoacetamide, and exchange buffer was replaced with digestion buffer containing 0.2% DCA and 50 mM ammonium bicarbonate. A ratio of 1:50 of sequencing grade modified trypsin (Promega, Madison, WI, USA) to substrate was then added, and the filter units were shaken at approximately 100 RPM for 12 hours at 37°C. Peptides were recovered by centrifugation and passage through the ultrafiltration membrane, and membranes were further washed with two 50-μL portions of 50 mM ammonium bicarbonate. The DCA in the combined filtrates was then extracted using ethyl acetate as previously described,[23] and peptides in the aqueous phase were dried by vacuum centrifugation.

Vitreous Humor Digestion

Bovine vitreous humor samples (≈200 μL) containing approximately 100 μg protein were dried by vacuum centrifugation and dissolved in 50 μL 8 M urea, 1.0 M Tris (pH 8.5), 8 mM $CaCl_2$, and 0.2 M methylamine. Samples were reduced by addition of 4 μL 0.2 M dithiothreitol and incubation at 50°C for 15 minutes, followed by alkylation through addition of 4 μL 0.5 M iodoacetamide and incubation at room temperature (RT) for

Investigative Ophthalmology & Visual Science

30 minutes in the dark. An additional 8 μL 0.2 M dithiothreitol was then added, samples were incubated for an additional 15 minutes at RT, and 94 μL water was added, followed by 40 μL 0.1 μg/μL trypsin. Digestion proceeded overnight at 37°C and then 10 μL formic acid was added to stop the reaction. Peptides were solid phase extracted using Sep-Pak Light C18 cartridges (Waters, Milford, MA, USA), and the final eluate was dried by vacuum concentration.

Liquid Chromatography–Mass Spectroscopy Analysis of Zonule and Vitreous Humor Digests

Samples were dissolved in water containing 5% formic acid and transferred to autosampler vials, and 4 μg of each zonule peptide digest (or 2 μg of each vitreous humor digest) was analyzed. The samples were injected at a flow rate of 5 μL/min onto an Acclaim PepMap 100-μm × 2-cm NanoViper 5-μm C18 trap (Thermo Fisher Scientific) using mobile phase A containing water and 0.1% formic acid. After 5 minutes, the trap was switched in-line with a PepMap RSLC C18, 2 μm, 75-μm × 25-cm EasySpray column fitted in an EasySpray nano electrospray source (Thermo Fisher Scientific) at 40°C. Peptides were eluted with a 90-minute gradient of 7.5%–30% mobile phase B containing acetonitrile and 0.1% formic acid at a flow rate of 0.3 μL/min. Peptides were analyzed using an Orbitrap Fusion mass spectrometer (Thermo Fisher Scientific). Survey scans were performed in the Orbitrap mass analyzer at a resolution of 120,000 with a scan range of 400–1500, maximum inject time of 50 ms, and automatic gain control (ACG) target of 2×10^5. The quadrupole was used to isolate ions for mass spectroscopy (MS)/MS scans with a 1.6-m/z isolation window, and fragmentation was performed by higher-energy collisional dissociation (HCD) with normalized collision energy of 35%. Top speed data-dependent MS/MS spectra were collected in parallel using the ion trap, with a maximum 35-ms inject time, single μscan, signal-to-noise ration (s/n) threshold = 2, minimum ion intensity threshold of 5000, and a maximum interval of 3 seconds between survey scans. Dynamic exclusion was performed with the monoisotopic precursor selection (MIPS) filter on, exclusion of +1 ions, 60-second exclusion time, exclusion mass tolerance of ±10 ppm, and count = 1. A file containing instrument settings, software version numbers, etc., is provided as Supplementary Materials S1.

Bioinformatics Analysis Pipeline

Conversion of RAW Files to MS2 Files. The open source Proteowizard toolkit[24] was used to convert Thermo RAW files into compressed text files using MSConvert via command line. An in-house Python program was used to convert information in the compressed text file into appropriately formatted MS2 files.[25] MS2 scans were extracted with a minimum ion count of 15 and minimum total absolute intensity of 100.

Database Searching. Databases were downloaded from Ensembl (www.ensembl.org, in the public domain) for bovine samples or from UniProt (www.uniprot.org, in the public domain) for human samples and processed with utilities available from www.ProteomicAnalysisWorkbench.com, in the public domain. Common contaminant sequences (179) were added before all sequences were reversed for peptide and protein error estimation using the target/decoy method.[26] The Ensembl bovine database (release 79, March 2015) had 22,118 protein sequences. The human database consisted of 20,207 UniProt reviewed canonical sequences (Swiss-Prot) downloaded July 2015. Searches were performed using Comet[27] version 2015.02 rev. 1 (human samples) or 2016.01 rev. 2 (bovine samples). Monoisotopic mass parent ion and fragment ion tolerances of 1.25 and 1.0005 Da were used, respectively. Other parameters were as follows: tryptic enzyme specificity, static modifications of +57 Da on cysteine residues, variable modifications of +16 Da on methionine residues (maximum of 2 modifications), and use of y- and b-ions in scoring.

Search Results Processing. The PAW analysis pipeline[28] was used to control peptide sequencing errors, infer protein identities from observed peptides, and provide quantitative protein abundance estimates. Acceptable peptide charge states were 2+, 3+, and 4+. Comet search scores were transformed into discriminant scores using functions similar to those used in PeptideProphet. Target and decoy discriminant scores were displayed as histograms and overlaid for interactive setting of score thresholds to filter peptide-spectral matches at an overall false discovery rate (FDR) of 3%.

Protein inference[29] used basic parsimony logic where proteins having indistinguishable peptide sets were combined into protein groups and proteins having peptide sets that were subset of other protein's peptide sets were removed. Protein inference was performed experiment-wide with additional requirements of a minimum of two distinct peptides per protein per biological sample applied after protein inference. In a final round of processing, straightforward extensions of parsimony principles were used to group together highly homologous proteins with mostly identical peptides. Protein FDRs, estimated from decoy protein matches, were less than 2%. These results were used for quantitative analyses using MS2 fragment ion intensity–weighted spectral counting.[30,31]

Determination of Contaminating Proteins

To more confidently determine the composition of the zonule, contaminating proteins from surrounding tissues have to be identified and excluded. It was assumed that the zonule would be composed predominantly of extracellular matrix (ECM) proteins. Comprehensive lists of ECM proteins for human and mouse have been compiled (http://matrisomeproject.mit.edu, in the public domain), and the lists of core and ECM-associated proteins for human were used to extract the corresponding protein sequence from UniProt. A FASTA database file of all human ECM proteins was constructed. For both human and bovine samples, the lists of identified proteins were used to extract separate FASTA database files for identified proteins. An in-house Python program was used to run a local installation of BLAST (ftp://ftp.ncbi.nlm.nih.gov/blast/executables/blast+/LATEST/, in the public domain) to determine the reciprocal best matches between the identified proteins and the human ECM proteins. Analysis of alignment scores was used to categorize likely matches to matrisome proteins from poor alignments between matrisome proteins and contaminating proteins. Once matrisome proteins were identified, their annotations were added to the results files. Common contaminant proteins and proteins not matching to matrisome ECM proteins were excluded from quantitative analysis. Extracellular matrix proteins constituted 90% of the bovine zonule sample and 82% of the human zonule sample. The total abundances of putative zonule proteins (using MS2 intensity–weighted spectral counts) were set to 100.00, and the relative abundance of the proteins within each sample was determined. Average protein abundances and their standard deviations were computed using standard Excel functions.

Unlike the human dataset, multiple proteins from the bovine dataset mapped to individual matrisome genes. This was because the bovine Ensemble protein database (unlike the human Swiss Prot database) contained multiple entries for protein isoforms of nearly identical sequence. To facilitate comparison to the human samples, the MS2 intensity–weighted spectral counts for all proteins mapping to the same matrisome gene symbol were summed together. Relative

Investigative Ophthalmology & Visual Science

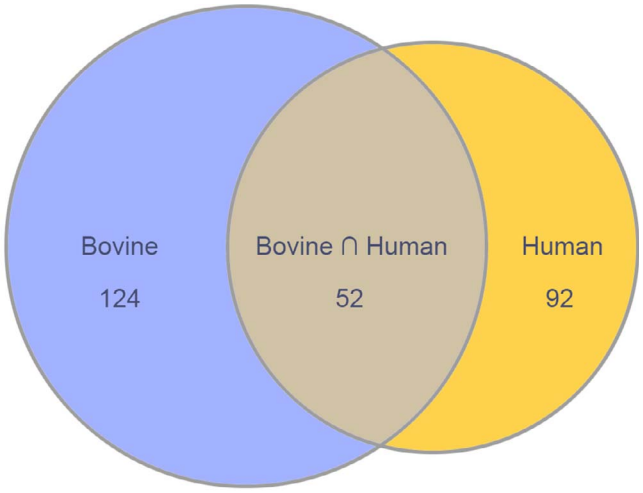

FIGURE 3. Components common to bovine and human zonulomes.

abundances within each sample by gene were computed as described above.

Full, annotated protein reports (Supplementary Materials S2, S3) and associated detailed peptide evidence files (Supplementary Materials S4, S5) for each experiment are included.

RESULTS

Comparison Between Human and Bovine Zonular Fibers

We began by comparing the protein composition of the human and bovine ciliary zonule (the zonulome). For this purpose, the human zonular sample was compared with the bovine equatorial zonule sample (see Materials and Methods). Our initial goal was to identify those proteins common to both, reasoning that protein conservation may imply important structural or signaling roles for the set of conserved proteins. Liquid chromatography–MS analysis of tryptic digests identified >1000 proteins, but, following removal of common contaminants and filtering against the matrisome database,[32,33] this number was reduced to 268 proteins (176 proteins in the bovine zonulome and 144 in the human). Fifty-two proteins were present in the zonulome of both species (Fig. 3). In terms of mass, >95% of the human and bovine zonules consisted of the proteins that were common to both species.

The matrisome[32,33] is the ensemble of >1000 genes that encode ECM components.[34] Two main classes of matrisomal proteins are defined: those constituting the core matrisome and those belonging to the group of matrisome-associated proteins. The core matrisome is further divided into three subcategories: ECM glycoproteins, collagens, and proteoglycans. The matrisome-associated protein category is also divided into three subcategories: ECM-affiliated proteins, ECM regulators, and secreted factors.

Of the six classes of matrisomal proteins, the two best represented by the number of identifications in the zonulome were glycoproteins (28 proteins in the human zonule and 53 in the bovine zonule) and ECM regulators (23 in humans and 26 in cows; (Figs. 4A, 4B). However, when the data were weighted according to protein abundance, based on MS2 intensity–weighted spectral counts, it was clear that in both cases the zonulome was dominated by glycoproteins (Figs. 4C, 4D). The nine most abundant glycoproteins in the human and bovine zonulome are ranked in Figure 5. The rankings for the two species were remarkably similar. The five most abundant proteins in either case were fibrillin-1 (FBN1), microfibrillar-associated protein 2 (MFAP2), latent-transforming growth factor β-binding protein-2 (LTBP2), EMILIN-1, and thrombospondin type-1 domain-containing protein 4 (THSD4, also known as ADAMTSL-6).

We used an orthogonal technique, confocal immunofluorescence, to verify the distribution of the four most abundant glycoproteins detected in the LC-MS analysis (FBN1, LTBP2, MFAP2, and EMILIN-1; Fig. 6). In sagittal sections of human ocular tissue, the zonule appeared as a system of fibers projecting from the pars plana region of the nonpigmented ciliary epithelium, fanning out as they approached the lens. At their midpoint, the fibers had a relatively large diameter but

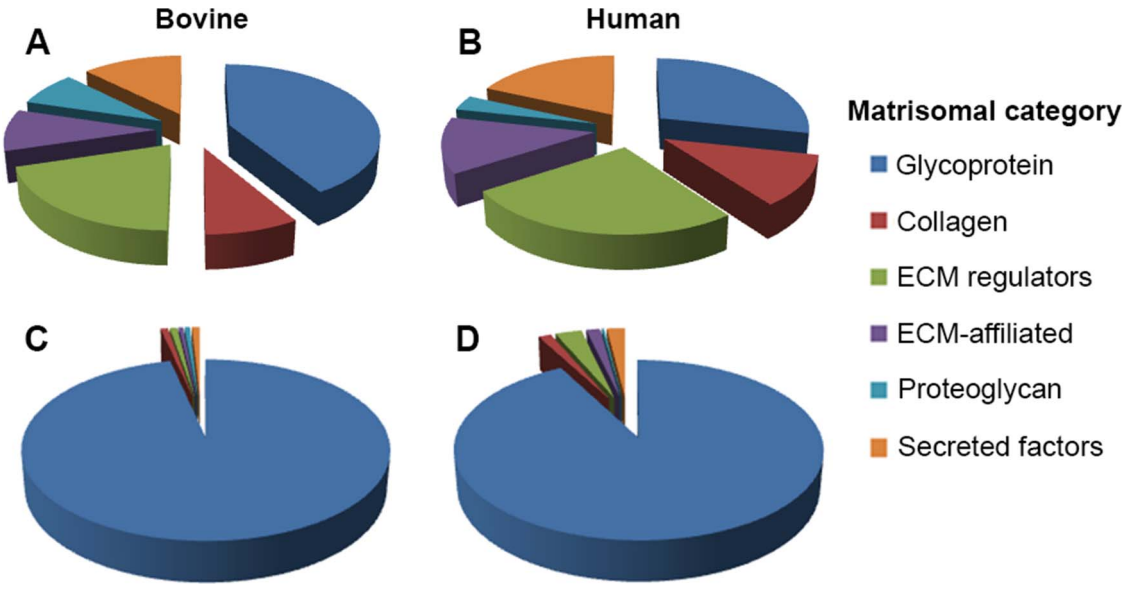

FIGURE 4. Overview of zonule composition in bovine (**A**, **C**) and human (**B**, **D**) samples. In terms of the number of proteins present (**A**, **B**), all six categories of matrisomal proteins are well represented in the zonulome. However, in terms of relative protein abundance, both zonulomes are composed predominantly of glycoproteins (**C**, **D**).

Investigative Ophthalmology & Visual Science

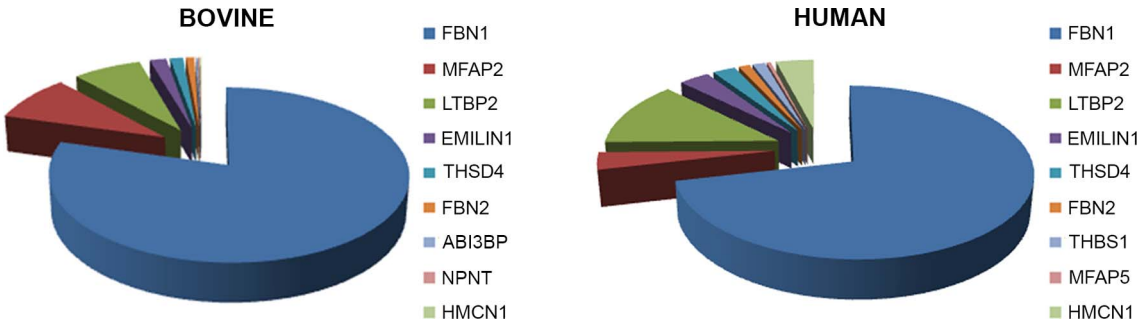

Figure 5. The ciliary zonule is rich in glycoproteins. Shown here is a ranking of the nine most-abundant glycoproteins, which together account for 95% of the bovine zonule and 89% of the human zonule.

near the lens surface, the large fibers divided to form smaller diameter fibers that inserted into the lens capsule (see insets in Fig. 6B). The three most abundant glycoproteins in the zonulome (FBN1, LTBP2, and MFAP2) labeled all zonular elements uniformly (Figs. 6A–C). In contrast, EMILIN-1 was present only in the large fibers (Fig. 6D).

Fibrillins and LTBPs comprise a superfamily of seven structurally related glycoproteins (FBN1-3 and LTBP1-4). All seven superfamily members were detected in the bovine zonule and only LTBP4 was absent from the human zonule (Fig. 7). The FBN/LTBP superfamily constituted 83.4% of the bovine zonule and 76.0% of the human zonule and represented the most abundant protein family in either zonulome. FBN1 was the most abundant individual protein, accounting for 63.49% and 75.57% of the protein in the human and bovine ciliary zonule, respectively.

The high representation of FBN/LTBP superfamily members in the zonule is consistent with the ocular phenotypes of syndromes resulting from mutations in those proteins. Mutations in *FBN1* underlie Marfan syndrome, a condition in which progressive lysis of the zonular fibers leads to ectopia lentis in most (71%) patients.[35] Mutations in *FBN1*[36] and *LTBP2*[37] have also been shown to cause Weill-Marchesani syndrome (types 2 and 3, respectively), which is a disease characterized by microspherophakia and ectopia lentis, in addition to systemic symptoms. Similarly, a highly penetrant ectopia lentis phenotype has been reported *Ltbp2*-null mice.[16] Together, these observations support the notion that FBN1 and LTBP2 play indispensable structural roles in the ciliary zonule. LTBPs, as their name implies, have the ability to bind and sequester latent forms of TGFβ in the ECM. Both the human and the bovine zonule contained relatively high levels of TGFβ-

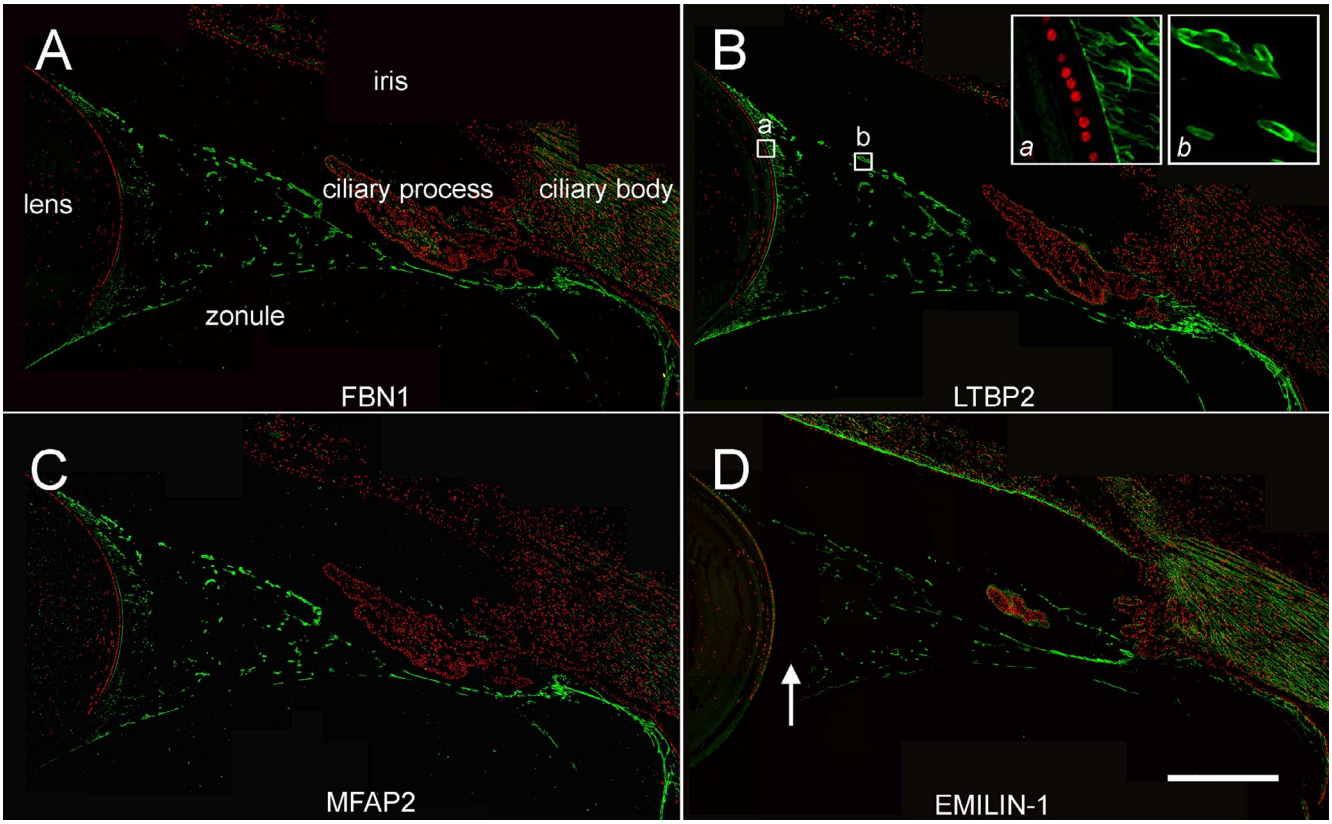

Figure 6. Immunofluorescence localization of glycoproteins in the human zonule. FBN1, LTBP2, and MFAP2 are distributed throughout the system of zonular fibers, including the small diameter fibers near the lens surface (inset *a* in **B**) and large diameter fibers at the midpoint of the zonular span (inset *b* in **B**). EMILIN-1 was absent from zonular fibers near the lens surface (*arrow* in **D**). *Scale bar* denotes 500 μm.

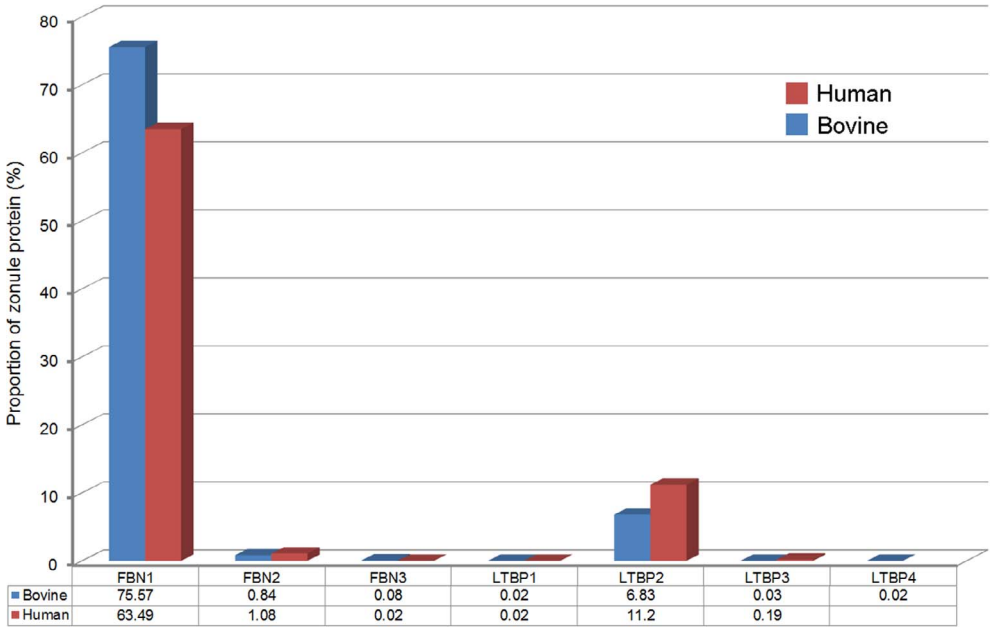

Figure 7. Fibrillin/LTBP superfamily expression in the ciliary zonule. All family members are present (with the exception of LTBP4 in the human zonule). FBN1 and LTBP2 are the most abundant components.

2 (lesser amounts of TGFβ-3 were also detected in the human sample). It is possible that LTBPs serve to target these molecules to the zonule. Curiously, LTBP2, by far the most abundant of the zonular LTBPs, is the only family member incapable of binding TGFβ so its role in the zonule and elsewhere is unresolved.[38]

Another class of proteins linked with inherited ectopia lentis (and the closely related condition ectopia lentis et pupillae, in which both the lens and the pupil are displaced) is the ADAMTSL family. ADAMTSLs share significant sequence similarity with the ADAMTS family of metalloproteases but lack the protease domain found in the latter. Mutations in *ADAMTSL-4* cause isolated ectopia lentis[21] and ectopia lentis et pupillae.[39] ADAMTSL-4 was detected in both the bovine and human zonules (at somewhat higher levels in the latter), as were ADAMTSL-1,-2 and -5. Unexpectedly, however, the most

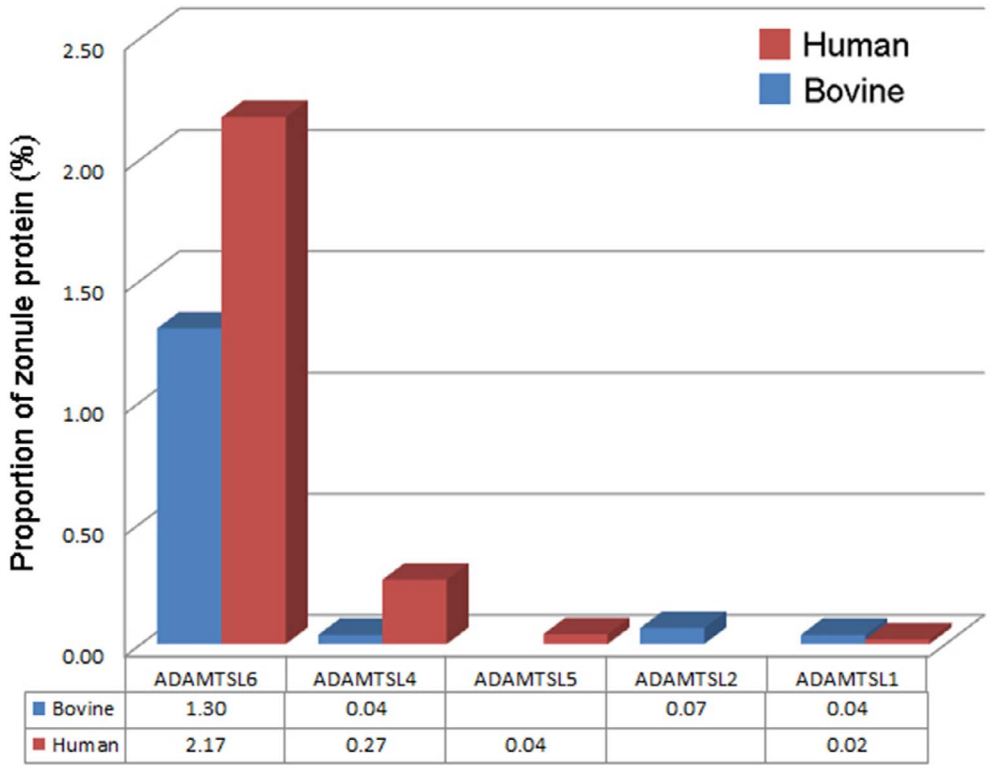

Figure 8. Expression of ADAMTSLs in the ciliary zonule.

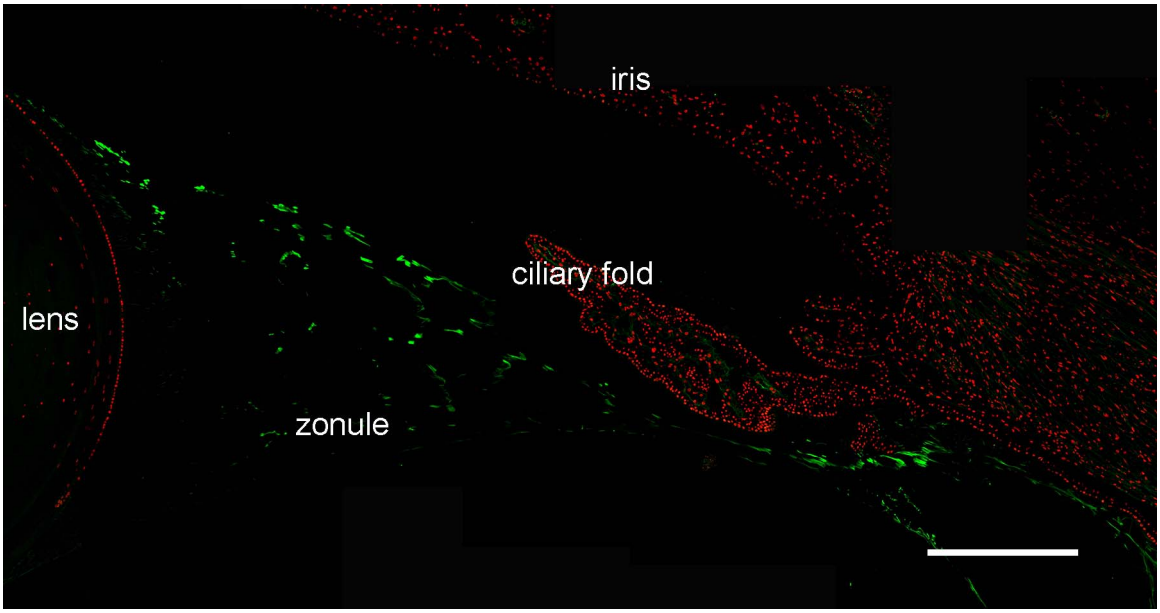

Figure 9. Expression of ADAMTSL-6/THSD4 (green) in the human ciliary zonule. Immunofluorescence is largely restricted to the large diameter fibers in the center of the zonular span and absent from small fibers at the lens surface (see Fig. 6B). *Scale bar* denotes 200 μm.

abundant member of the family was ADAMTSL-6 (also known as THSD4), which, in the human zonule, accounted for >2% of the total protein (Figs. 5, 8). We used immunofluorescence to verify the expression of ADAMTSL-6 in the human eye (Fig. 9). ADAMTSL-6 was strongly expressed in the large diameter fibers in a similar fashion to EMILIN-1 (Fig. 6D). In vitro studies suggest that ADAMTSL-6 can bind directly to FBN1, promoting the assembly of fibrillin-rich ECM.[40]

A number of protease inhibitors were detected in the zonule, including several members of the SERPIN family, but the most abundant inhibitor, particularly in the human sample, was TIMP3 (Fig. 10). The TIMPs are widely expressed endogenous inhibitors of matrix metalloproteinases. TIMP3 is unusual in that it also has antiangiogenic properties. In the eye, mutations in *TIMP3* have been linked to Sorsby's Fundus dystrophy.[41] The only protease detected in both the human and bovine zonule was cathepsin D, a lysosomal aspartic endopeptidase that may also be secreted from cells.[42]

Each zonular fiber is composed of bundles of hundreds or thousands of individual microfibrils.[9] Although microfibrils are

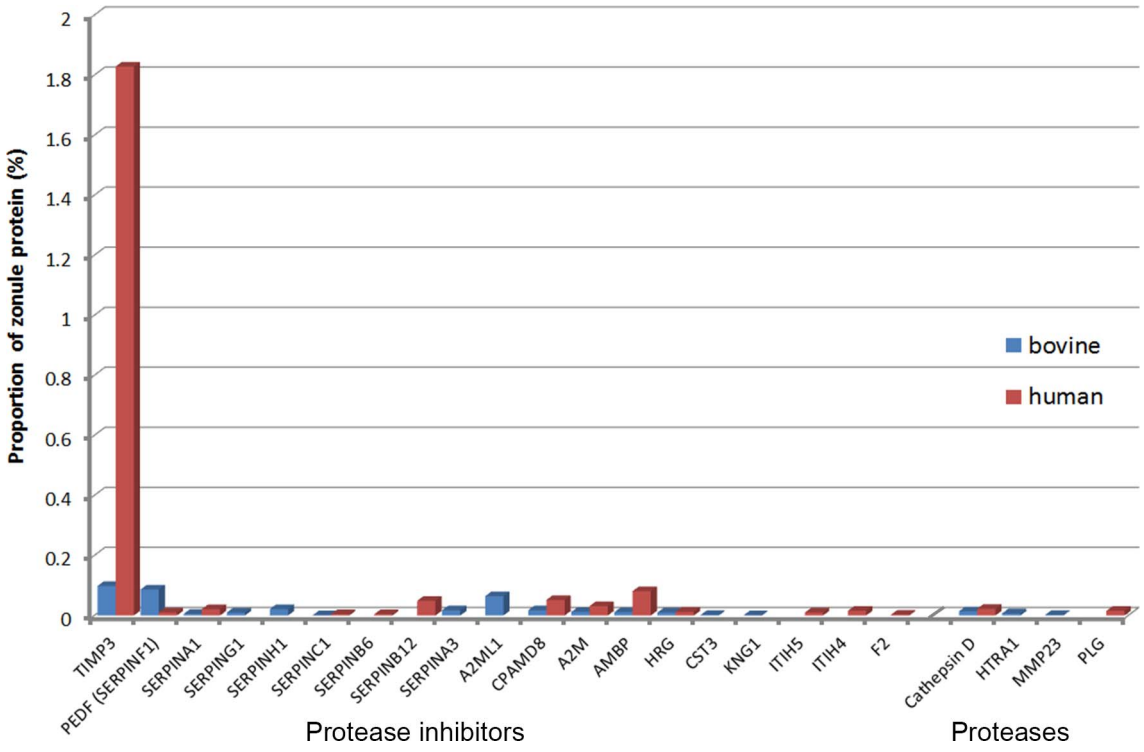

Figure 10. Expression of proteases/protease inhibitors in the ciliary zonule.

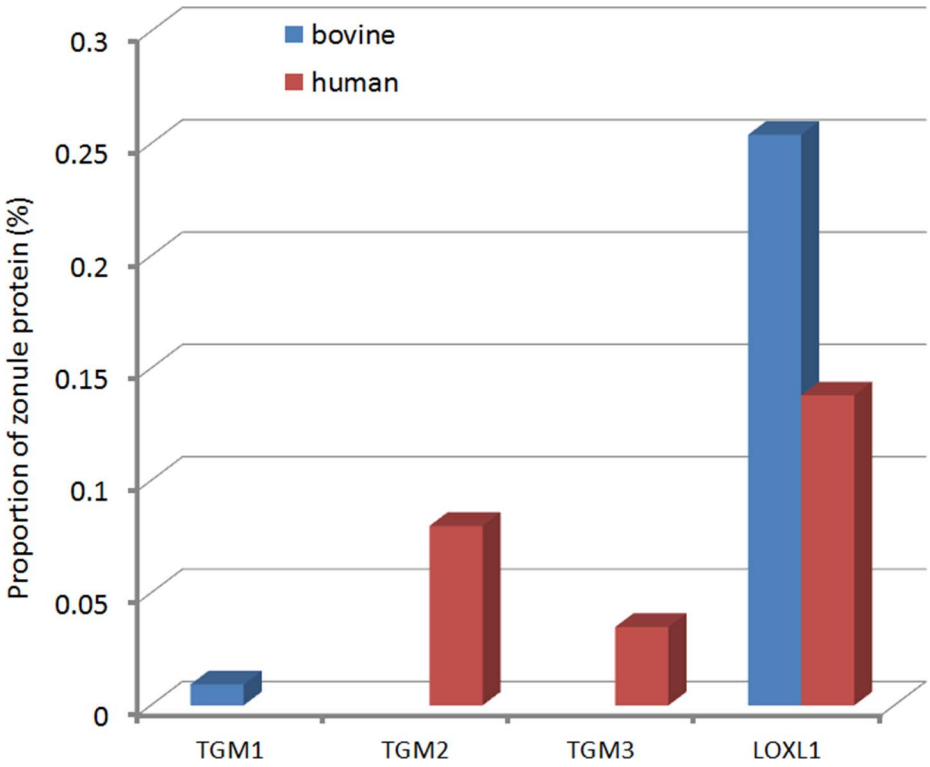

Figure 11. Expression of crosslinking enzymes (transglutaminases and lysyloxidase-like 1) in the ciliary zonule.

stiff structures,[10] the zonular fibers themselves are quite elastic. Work on model systems suggest that the material properties of microfibrillar networks are shaped by both nonreducible crosslinks and disulfide bonds.[11] We examined human and bovine zonules for the presence of known crosslinking enzymes that might play a role in bundling of microfibrils. Several transglutaminases (TGM1-3) were detected, but the most abundant crosslinker detected was lysyl oxidase-like 1 (LOXL1; Fig. 11). Transglutaminase-derived crosslinks have been identified previously in fibrillin microfibrils and may be important in the zonule.[43] The presence of LOXL1 is intriguing because variants in the *LOXL1* gene have been shown to predispose to exfoliation syndrome.[44] Exfoliation syndrome is a condition in which disintegration of the zonular fibers and unscheduled production of matrix components results in formation of fibrillar aggregates that can clog the outflow pathways of the eye, leading to exfoliation glaucoma.[45] The best characterized substrates for LOXL1 are lysine residues in elastin.[46] Elastin polymerization requires oxidative deamination of lysine residues. The resulting aldehyde groups condense spontaneously, forming covalent crosslinkages. Given its demonstrated role in elastin polymerization, it is curious that LOXL1 is such a prominent component of the elastin-free ciliary zonule. One explanation may be that fibrillin or other zonule components serve as substrates for LOXL1. The availability of mice deficient in LOXL1[46] should allow us to test whether LOXL1 has a role in crosslinking microfibrils.

The expression of collagens, secreted factors, and proteoglycans was compared in the human and bovine zonular samples (Supplementary Tables S1, S2). Only trace amounts of collagen were detected, of which the most abundant were COL2A1 and COL9A2. COL4 and COL18, components of basement membranes, were also detected and may represent contamination from the lens capsule or the inner limiting membrane covering the basal surface of the nonpigmented ciliary epithelium.

Several secreted factors were identified in the zonular samples. MEGF6, shown to interact via its EGF domains with MFAP5,[47] was one of the most abundant. Immune components, such as CXCL14 and EGFL7, were identified in the human but not bovine zonule. This may reflect the fact that the human samples were largely from middle-aged individuals (Table), whereas the bovine samples were from young animals. Similarly, the presence of IL17D in human samples may indicate ongoing inflammatory reactions in the aged human eyes. CXCL14 is a chemokine implicated in the recruitment of immune cells in all types of inflammatory conditions.

Proteoglycans were not prominent zonule components in either species, although in the bovine zonule, opticin (OPT) was detected at moderate levels. Opticin was much more abundant in the bovine hyaloid zonule (see below).

Comparison Between the Bovine Equatorial Zonule, Hyaloid Zonule, and Vitreous Humor

Unlike the bovine zonule (where members of a single glycoprotein family, the FBN/LTBP family, accounted for >80% of the protein), the composition of the vitreous was not dominated by a restricted set of super abundant proteins (Supplementary Material S3). Among the more abundant vitreous proteins were broad spectrum protease inhibitors (A2ML1, A2M, CPMD8, CST3, and SERPING1), collagens (COL9A2, COL18A1, and COL2A1), fibulins (FBLN1, FBLN2, and FBNL3), the proteoglycans OPT and HSPG2, and WNT signaling components SFRP2 and SFRP3. FBN1, the most abundant single component in the equatorial zonule, accounted for only 2.5% of the protein in the vitreous sample.

Recent proteomic analyses of human vitreous humor[48–50] have identified many hundreds of protein components, of which a core set of 231 proteins were detected in all studies. In

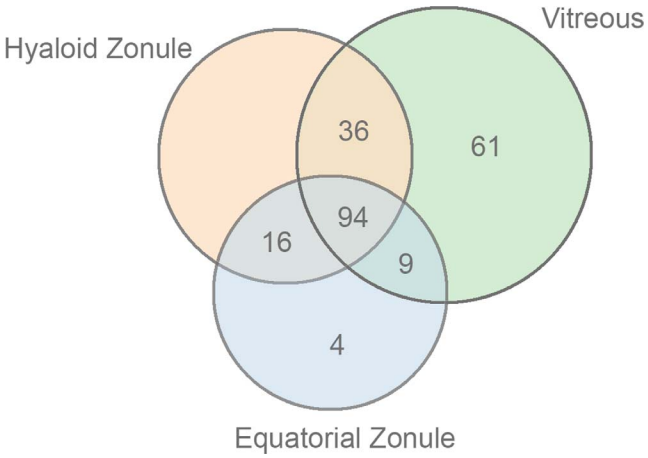

Figure 12. Overlapping distribution of matrisome proteins in samples from the bovine equatorial zonule, hyaloid zonule, and vitreous humor.

the present study, after filtering against the matrisome database, we identified 200 components of the bovine vitreous. Comparing the bovine vitreous proteome with that of the equatorial and hyaloid zonular samples, it was evident that the zonular samples were quite distinct from the vitreous sample (Figs. 12, 13). Proteins such as MFAP2 and FBN2, for example, were almost undetectable in the vitreous but relatively abundant in the zonular samples.

The hyaloid zonule is associated with the vitreous face, and it is possible that during dissection, the hyaloid sample might have been contaminated with proteins emanating from the vitreous. If we assume that the hyaloid zonule has a similar basic composition to the equatorial zonule, then vitreous contamination should lead to values for relative protein abundance that were intermediate between the vitreous and equatorial zonule values. Although such instances were certainly observed, there were also many examples where the abundance of a protein in the hyaloid zonule significantly exceeded (by orders of magnitude) that of the vitreous or the equatorial zonule. Such proteins are likely to be unique to, or significantly enriched in, the hyaloid zonule sample. The set of hyaloid-enriched proteins included OPT, A3i3bp, cochlin, and the collagens COL2A1, COL11A1, COL5A3, and COL5A2 (Fig. 13).

Histograms showing relative abundance of each class of matrisomal proteins in the bovine samples are included as Supplementary Figures S6–S12.

Discussion

The ciliary zonule plays a key role in ocular function, centering the lens on the optical axis and transmitting the forces that mold its shape during accommodation. The zonule is adversely affected in several pathologic conditions, including exfoliation syndrome, homocystinuria, and Marfan syndrome. To understand how and why the zonule is compromised in these diseases, a detailed analysis of its composition is necessary.

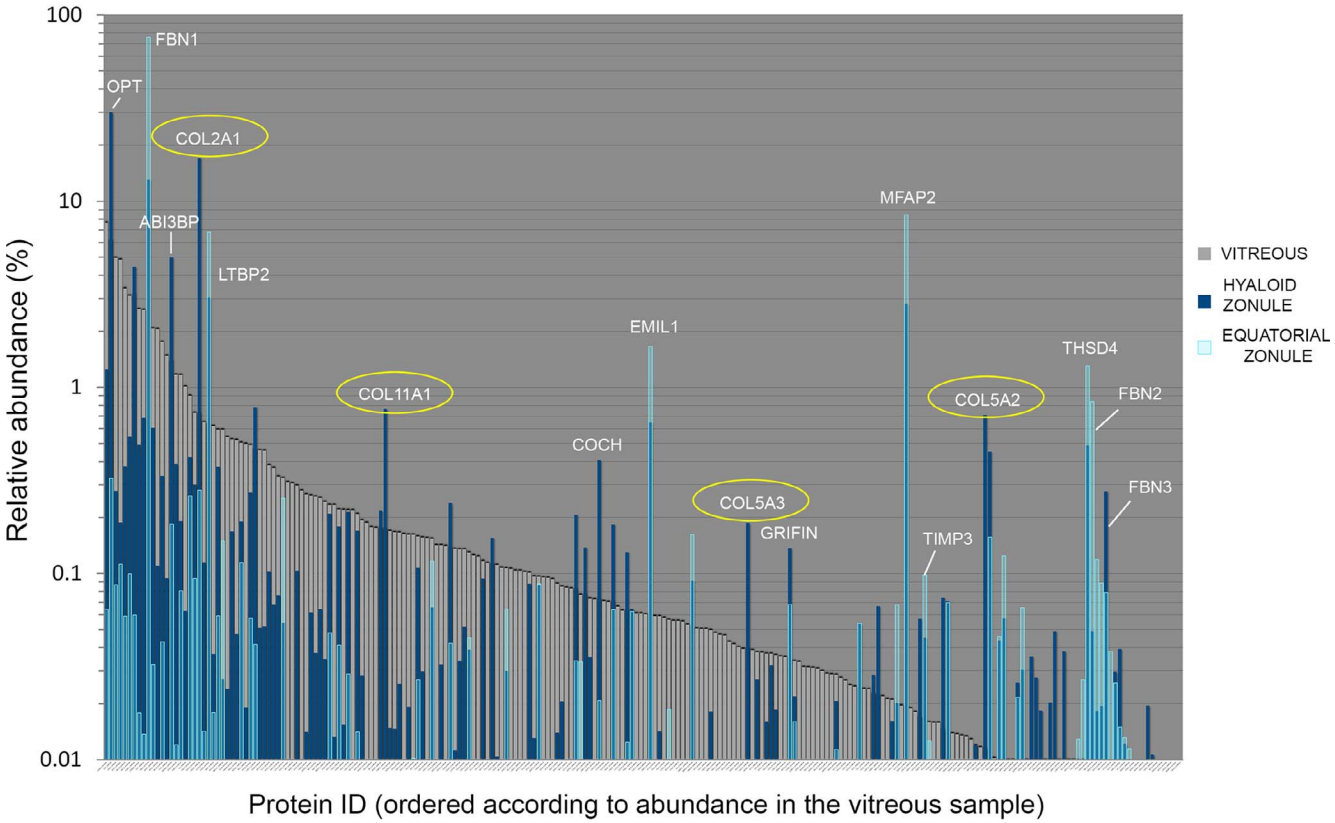

Figure 13. Protein composition of samples from the bovine vitreous humor (*gray*), equatorial zonule (*light blue*), and hyaloid zonule (*dark blue*). Proteins are ordered according to their abundance in the vitreous humor sample. Some proteins are relatively abundant in all three samples; others, such as THSD4, are abundant in the zonular samples but barely detectable in the vitreous. Examples of zonule-enriched proteins are labeled in *white*. Three classes of fibrillary collagen (type 2A, 11A, and 5A; circled in *yellow*) are significantly overrepresented in the hyaloid zonule sample compared with the equatorial zonule or vitreous. Note that opticin (OPT) accounts for 30% of the hyaloid zonule but was barely detectable in the equatorial zonule.

Investigative Ophthalmology & Visual Science

Microfibrils (the main structural elements of the zonule) are ubiquitous components of the ECM but questions remain regarding their organization, synthesis, and role as signaling hubs. The ciliary zonule, a readily accessible, cell-free system composed of bundled microfibrils, represents a useful model system in which to gain insights into microfibril organization.

The composition of the equatorial zonule was broadly similar in humans and cows, and the set of 52 proteins identified in both samples accounted for >95% of the mass in either case. The fact that the human samples were from middle-aged individuals, whereas the bovine samples were from young animals, might in part explain why more proteins were identified in the bovine zonulome (176 vs. 144). The bovine samples were also obtained shortly after death, whereas the human samples were obtained 24–48 hours postmortem. It is possible that labile proteins were lost from the human samples during the postmortem period.

In both humans and cows, the zonule consisted of a microfibril backbone comprised primarily of fibrillin and a relatively restricted set of glycoproteins. LTBP2, a fibrillin-like protein implicated in autosomal recessive Weill-Marchesani syndrome type 3 (WMS3: MIM#614819[37]), was a surprisingly abundant component, comprising ≈10% of the total zonular protein. There are three fibrillin genes in humans and the presence of all three proteins was confirmed in the zonulome, consistent with earlier observations.[15] FBN2, the second most abundant fibrillin in the zonule, is synthesized early in development and is essential for normal zonule formation in mice.[51] Immunolocalization studies have previously failed to detect FBN2 in the adult zonule, but its presence in the human and bovine zonulome suggests that FBN2 epitopes may become inaccessible to antibody staining during postnatal development, as reported in other systems.[52]

Several proteins implicated in TGFβ signaling were detected in the zonule. Despite its name, latent TGFβ binding protein 2 (LTBP2) is not a bona fide TGFβ-binding protein, but two other family members, LTBP1 and LTBP3, were detected in the zonulome. In other systems, LTBP1 and LTBP3 facilitate the sequestration (and release) of TGFβ in the ECM through interaction with FBN1 and other components.[53] Of note, both TGFβ2 and TGFβ3 ligands were detected in the human zonulome. Another protein with a potential role in modulating TGFβ signaling was EMILIN-1, a prominent component of the human and bovine zonulome. EMILIN-1 has been shown to inhibit TGFβ signaling by binding to pro-TGFβ precursor and preventing its furin-mediated maturation.[54] EMILIN-1–deficient mice have hypertension, but no ocular phenotype has been noted.[55] EMILINs were originally identified as elastic fiber components located at the interface between microfibrils and the underlying elastin core.[56] More recent studies have suggested that they associate directly with microfibrils.[57] Because zonular fibers insert into the lens capsule directly above the lens germinative zone (the region of the lens epithelium containing the mitotically active cell population), TGFβ or other growth factors sequestered in the zonule are well placed to influence the growth of the lens directly. It is also possible that the cyclical stretching of the zonule during accommodation might serve to release bound factors from the surface of zonular fibers.

One of the novel (and abundant) proteins detected in our study was ADAMTSL-6 (THSD4). ADAMTS proteins and ADAMTSL proteins have well-documented roles in ocular biology and pathology.[58] ADAMTSL-6 has not been identified previously in the zonule but, in other systems, is known to bind to the N terminus of FBN1, where it may promote microfibril formation.[40] Among the proteins that we expected to detect in the zonulome, but did not, was ADAMTS10; ADAMTS10 mutations underlie Weill-Marchesani syndrome type 1 (WMS1). Ectopia lentis is commonly observed in WMS1, implying a mechanical defect in the ciliary zonule. Clinically, WMS1 is indistinguishable from WMS2 and WMS3, syndromes caused by mutations in *FBN1* and *LTBP2* respectively, genes encoding two of the most abundant zonular proteins. Immunoelectron microscopy studies have previously suggested that ADAMTS10 is abundant in the human ciliary zonule[59] so its absence from the proteome is perplexing.

A striking feature of the zonulome in human and cows was the presence of a diverse set of protease inhibitors, the most abundant in humans being TIMP3. The zonule is known to be exquisitely sensitive to proteolysis. Before the introduction of modern cataract surgery, ophthalmologists removed the cataractous lens in a single piece, a procedure facilitated by brief exposure to dilute solutions of α-chymotrypsin, which served to lyse the zonule and release the lens from the eye. The presence of TIMP3 and other protease inhibitors may help explain the evident durability of the zonule, despite lifelong exposure to matrix metalloproteinases and other proteases present in the ocular humors.[60]

The hyaloid zonule is intimately associated with the anterior face of the vitreous. During ophthalmic surgery, the vitreous face behaves, physically, as if it were a distinct membrane (the "hyaloid membrane"). Ophthalmologists take great care not to damage the hyaloid membrane during surgical procedures, lest the contents of the vitreous leak. The current study may provide some clues as to the nature of the hyaloid membrane. First, it is apparent that the hyaloid membrane is reinforced by the presence of a meshwork of fibrillin-rich microfibrils, the hyaloid zonule. During dissection of the hyaloid zonule it is likely that proteins from the anterior-most region of the vitreous were coisolated. The hyaloid zonule sample was characterized by the presence of high concentrations of opticin, consistent with previous immunolocalization studies of opticin in human eyes.[61] Our analysis also suggested that the hyaloid sample was enriched in fibrillar collagens (especially COL2A1, COL5A2, COL5A3, and COL11A1), which were detected elsewhere in the vitreous but at much lower concentrations. Interestingly, mutations in COL2A1 and COL11A1 result in Stickler syndrome, a condition characterized by vitreous pathology. In Stickler syndrome type 1 (caused by COL2A1 mutations), a "membranous vitreous" is often observed; whereas in Stickler syndrome type 2 (COL11A1) a "beaded vitreous" is observed.[62] In each case the anterior face of the vitreous appears to be compromised. Thus, the phenotypes in Stickler syndrome are consistent with a model in which fibrillar collagens form part of a meshwork (along with fibrillin-rich microfibrils and opticin) that defines and supports the vitreous face.

One question arising from the current study is why such an unassuming structure as the ciliary zonule should require a proteome with fifty or more components? In other settings, it is evident that microfibril scaffolds, decorated with latent growth factors, serve as both mechanosensors and signaling hubs.[63] Perhaps the zonule has analogous functions in the eye. The pleitropic ocular effects of mutations in zonular genes (which include congenital glaucoma, cataract, ectopia lentis, and microspherophakia) are consistent with the notion that the role of the ciliary zonule is not solely to secure the lens in place.

Acknowledgments

The authors thank Dirk Hubmacher of the Cleveland Clinic for coining the phrase "zonulome." Cow eyes were generously provided by Trenton Processing. The authors are particularly grateful to the staff of Mid-America Transplant, St. Louis, MO, USA, for providing ocular tissue and to the donors and their families.

Investigative Ophthalmology & Visual Science

Without their generosity, this project would not have been possible.

Supported by National Institutes of Health grants R01 EY024607 (SB), P30 EY02687, Oregon Health and Science University (OHSU) Core grants P30 EY010572 and P30 CA069533, shared instrument grant S10OD012246, the National Marfan Foundation, and an unrestricted grant to the Department of Ophthalmology and Visual Sciences from Research to Prevent Blindness.

Disclosure: **A. De Maria**, None; **P.A. Wilmarth**, None; **L.L. David**, None; **S. Bassnett**, None

References

1. Zinn JG. *Descriptio Anatomica Oculi Humani Iconibus Illustrata*. Gottingen: Viduam B: Abrami Vandenhoeck; 1755.
2. Weeber HA, van der Heijde RG. Internal deformation of the human crystalline lens during accommodation. *Acta Ophthalmol*. 2008;86:642–647.
3. Shi Y, Tu Y, De Maria A, Mecham RP, Bassnett S. Development, composition, and structural arrangements of the ciliary zonule of the mouse. *Invest Ophthalmol Vis Sci*. 2013;54: 2504–2515.
4. Bernal A, Parel JM, Manns F. Evidence for posterior zonular fiber attachment on the anterior hyaloid membrane. *Invest Ophthalmol Vis Sci*. 2006;47:4708–4713.
5. Assia EI, Apple DJ, Morgan RC, Legler UF, Brown SJ. The relationship between the stretching capability of the anterior capsule and zonules. *Invest Ophthalmol Vis Sci*. 1991;32: 2835–2839.
6. Fisher RF. The ciliary body in accommodation. *Trans Ophthalmol Soc U K*. 1986;105(Pt 2):208–219.
7. Michael R, Mikielewicz M, Gordillo C, Montenegro GA, Pinilla Cortes L, Barraquer RI. Elastic properties of human lens zonules as a function of age in presbyopes. *Invest Ophthalmol Vis Sci*. 2012;53:6109–6114.
8. van Alphen GW, Graebel WP. Elasticity of tissues involved in accommodation. *Vision Res*. 1991;31:1417–1438.
9. Raviola G. The fine structure of the ciliary zonule and ciliary epithelium. With special regard to the organization and insertion of the zonular fibrils. *Invest Ophthalmol Vis Sci*. 1971;10:851–869.
10. Sherratt MJ, Baldock C, Haston JL, et al. Fibrillin microfibrils are stiff reinforcing fibres in compliant tissues. *J Mol Biol*. 2003;332:183–193.
11. Thurmond F, Trotter J. Morphology and biomechanics of the microfibrillar network of sea cucumber dermis. *J Exp Biol*. 1996;199:1817–1828.
12. Sakai LY, Keene DR, Engvall E. Fibrillin, a new 350-kD glycoprotein, is a component of extracellular microfibrils. *J Cell Biol*. 1986;103:2499–2509.
13. Gibson MA, Hughes JL, Fanning JC, Cleary EG. The major antigen of elastin-associated microfibrils is a 31-kDa glycoprotein. *J Biol Chem*. 1986;261:11429–11436.
14. Cain SA, Morgan A, Sherratt MJ, Ball SG, Shuttleworth CA, Kielty CM. Proteomic analysis of fibrillin-rich microfibrils. *Proteomics*. 2006;6:111–122.
15. Hubmacher D, Reinhardt DP, Plesec T, Schenke-Layland K, Apte SS. Human eye development is characterized by coordinated expression of fibrillin isoforms. *Invest Ophthalmol Vis Sci*. 2014;55:7934–7944.
16. Inoue T, Ohbayashi T, Fujikawa Y, et al. Latent TGF-beta binding protein-2 is essential for the development of ciliary zonule microfibrils. *Hum Mol Genet*. 2014;23:5672–5682.
17. Collin GB, Hubmacher D, Charette JR, et al. Disruption of murine Adamtsl4 results in zonular fiber detachment from the lens and in retinal pigment epithelium dedifferentiation. *Hum Mol Genet*. 2015;24:6958–6974.
18. Buschmann W, Linnert D, Hofmann W, Gross A. The tensile strength of human zonule and its alteration with age (author's transl) [in German]. *Albrecht Von Graefes Arch Klin Exp Ophthalmol*. 1978;206:183–190.
19. Sangal N, Chen TC. Cataract surgery in pseudoexfoliation syndrome. *Semin Ophthalmol*. 2014;29:403–408.
20. Schlotzer-Schrehardt U, Naumann GO. A histopathologic study of zonular instability in pseudoexfoliation syndrome. *Am J Ophthalmol*. 1994;118:730–743.
21. Ahram D, Sato TS, Kohilan A, et al. A homozygous mutation in ADAMTSL4 causes autosomal-recessive isolated ectopia lentis. *Am J Hum Genet*. 2009;84:274–278.
22. Neuhann TM, Stegerer A, Riess A, et al. ADAMTSL4-associated isolated ectopia lentis: further patients, novel mutations and a detailed phenotype description. *Am J Med Genet A*. 2015; 167A:2376–2381.
23. Erde J, Loo RR, Loo JA. Enhanced FASP (eFASP) to increase proteome coverage and sample recovery for quantitative proteomic experiments. *J Proteome Res*. 2014;13:1885–1895.
24. Chambers MC, Maclean B, Burke R, et al. A cross-platform toolkit for mass spectrometry and proteomics. *Nat Biotechnol*. 2012;30:918–920.
25. McDonald WH, Tabb DL, Sadygov RG, et al. MS1, MS2, and SQT-three unified, compact, and easily parsed file formats for the storage of shotgun proteomic spectra and identifications. *Rapid Commun Mass Spectrom*. 2004;18:2162–2168.
26. Elias JE, Gygi SP. Target-decoy search strategy for increased confidence in large-scale protein identifications by mass spectrometry. *Nat Methods*. 2007;4:207–214.
27. Eng JK, Jahan TA, Hoopmann MR. Comet: an open-source MS/MS sequence database search tool. *Proteomics*. 2013;13:22–24.
28. Wilmarth PA, Riviere MA, David LL. Techniques for accurate protein identification in shotgun proteomic studies of human, mouse, bovine, and chicken lenses. *J Ocul Biol Dis Inform*. 2009;2:223–234.
29. Nesvizhskii AI, Aebersold R. Interpretation of shotgun proteomic data: the protein inference problem. *Mol Cell Proteomics*. 2005;4:1419–1440.
30. Krey JF, Wilmarth PA, Shin JB, et al. Accurate label-free protein quantitation with high- and low-resolution mass spectrometers. *J Proteome Res*. 2014;13:1034–1044.
31. Spinelli KJ, Klimek JE, Wilmarth PA, et al. Distinct energy metabolism of auditory and vestibular sensory epithelia revealed by quantitative mass spectrometry using MS2 intensity. *Proc Natl Acad Sci U S A*. 2012;109:E268–E277.
32. Naba A, Clauser KR, Ding H, Whittaker CA, Carr SA, Hynes RO. The extracellular matrix: tools and insights for the "omics" era. *Matrix Biol*. 2016;49:10–24.
33. Hynes RO, Naba A. Overview of the matrisome—an inventory of extracellular matrix constituents and functions. *Cold Spring Harb Perspect Biol*. 2012;4:a004903.
34. Naba A, Clauser KR, Hoersch S, Liu H, Carr SA, Hynes RO. The matrisome: in silico definition and in vivo characterization by proteomics of normal and tumor extracellular matrices. *Mol Cell Proteomics*. 2012;11:M111014647.
35. Fuchs J. Marfan syndrome and other systemic disorders with congenital ectopia lentis. A Danish national survey. *Acta Paediatr*. 1997;86:947–952.
36. Faivre L, Gorlin RJ, Wirtz MK, et al. In frame fibrillin-1 gene deletion in autosomal dominant Weill-Marchesani syndrome. *J Med Genet*. 2003;40:34–36.
37. Haji-Seyed-Javadi R, Jelodari-Mamaghani S, Paylakhi SH, et al. LTBP2 mutations cause Weill-Marchesani and Weill-Marchesani-like syndrome and affect disruptions in the extracellular matrix. *Hum Mutat*. 2012;33:1182–1187.

38. Saharinen J, Keski-Oja J. Specific sequence motif of 8-Cys repeats of TGF-beta binding proteins, LTBPs, creates a hydrophobic interaction surface for binding of small latent TGF-beta. *Mol Biol Cell*. 2000;11:2691–2704.
39. Christensen AE, Fiskerstrand T, Knappskog PM, Boman H, Rodahl E. A novel ADAMTSL4 mutation in autosomal recessive ectopia lentis et pupillae. *Invest Ophthalmol Vis Sci*. 2010;51:6369–6373.
40. Tsutsui K, Manabe R, Yamada T, et al. ADAMTSL-6 is a novel extracellular matrix protein that binds to fibrillin-1 and promotes fibrillin-1 fibril formation. *J Biol Chem*. 2010;285:4870–4882.
41. Weber BH, Vogt G, Pruett RC, Stohr H, Felbor U. Mutations in the tissue inhibitor of metalloproteinases-3 (TIMP3) in patients with Sorsby's fundus dystrophy. *Nat Genet*. 1994;8:352–356.
42. Benes P, Vetvicka V, Fusek M. Cathepsin D—many functions of one aspartic protease. *Crit Rev Oncol Hematol*. 2008;68:12–28.
43. Qian RQ, Glanville RW. Alignment of fibrillin molecules in elastic microfibrils is defined by transglutaminase-derived cross-links. *Biochemistry*. 1997;36:15841–15847.
44. Thorleifsson G, Magnusson KP, Sulem P, et al. Common sequence variants in the LOXL1 gene confer susceptibility to exfoliation glaucoma. *Science*. 2007;317:1397–1400.
45. Ritch R. Ocular and systemic manifestations of exfoliation syndrome. *J Glaucoma*. 2014;23:S1–S8.
46. Liu X, Zhao Y, Gao J, et al. Elastic fiber homeostasis requires lysyl oxidase-like 1 protein. *Nat Genet*. 2004;36:178–182.
47. Penner AS, Rock MJ, Kielty CM, Shipley JM. Microfibril-associated glycoprotein-2 interacts with fibrillin-1 and fibrillin-2 suggesting a role for MAGP-2 in elastic fiber assembly. *J Biol Chem*. 2002;277:35044–35049.
48. Yee KM, Feener EP, Madigan M, et al. Proteomic analysis of embryonic and young human vitreous. *Invest Ophthalmol Vis Sci*. 2015;56:7036–7042.
49. Murthy KR, Goel R, Subbannayya Y, et al. Proteomic analysis of human vitreous humor. *Clin Proteomics*. 2014;11:29.
50. Semba RD, Enghild JJ, Venkatraman V, Dyrlund TF, Van Eyk JE. The Human Eye Proteome Project: perspectives on an emerging proteome. *Proteomics*. 2013;13:2500–2511.
51. Shi Y, Tu Y, Mecham RP, Bassnett S. Ocular phenotype of Fbn2-null mice. *Invest Ophthalmol Vis Sci*. 2013;54:7163–7173.
52. Charbonneau NL, Jordan CD, Keene DR, et al. Microfibril structure masks fibrillin-2 in postnatal tissues. *J Biol Chem*. 2010;285:20242–20251.
53. Robertson IB, Horiguchi M, Zilberberg L, Dabovic B, Hadjiolova K, Rifkin DB. Latent TGF-beta-binding proteins. *Matrix Biol*. 2015;47:44–53.
54. Zacchigna L, Vecchione C, Notte A, et al. Emilin1 links TGF-beta maturation to blood pressure homeostasis. *Cell*. 2006;124:929–942.
55. Zanetti M, Braghetta P, Sabatelli P, et al. EMILIN-1 deficiency induces elastogenesis and vascular cell defects. *Mol Cell Biol*. 2004;24:638–650.
56. Bressan GM, Daga-Gordini D, Colombatti A, Castellani I, Marigo V, Volpin D. Emilin, a component of elastic fibers preferentially located at the elastin-microfibrils interface. *J Cell Biol*. 1993;121:201–212.
57. Schiavinato A, Keene DR, Wohl AP, et al. Targeting of EMILIN-1 and EMILIN-2 to fibrillin microfibrils facilitates their incorporation into the extracellular matrix. *J Invest Dermatol*. 2016;136:1150–1160.
58. Hubmacher D, Apte SS. ADAMTS proteins as modulators of microfibril formation and function. *Matrix Biol*. 2015;47:34–43.
59. Kutz WE, Wang LW, Bader HL, et al. ADAMTS10 protein interacts with fibrillin-1 and promotes its deposition in extracellular matrix of cultured fibroblasts. *J Biol Chem*. 2011;286:17156–17167.
60. Sivak JM, Fini ME. MMPs in the eye: emerging roles for matrix metalloproteinases in ocular physiology. *Prog Retin Eye Res*. 2002;21:1–14.
61. Ramesh S, Bonshek RE, Bishop PN. Immunolocalisation of opticin in the human eye. *Br J Ophthalmol*. 2004;88:697–702.
62. Snead MP, McNinch AM, Poulson AV, et al. Stickler syndrome, ocular-only variants and a key diagnostic role for the ophthalmologist. *Eye (Lond)*. 2011;25:1389–1400.
63. Sengle G, Sakai LY. The fibrillin microfibril scaffold: a niche for growth factors and mechanosensation? *Matrix Biol*. 2015;47:3–12.

Investigative Ophthalmology & Visual Science